ELSEVIER

25 May 2001

Chemical Physics Letters 340 (2001) 71–76

CHEMICAL PHYSICS LETTERS

www.elsevier.nl/locate/cplett

Chlorine atom spin–orbit branching ratios and total absolute reaction cross-sections for the H + DCl → HD + Cl reaction

Alexander Hanf, Almuth Läuter, Dhanya Suresh [1], Hans-Robert Volpp *, Jürgen Wolfrum

Physikalisch-Chemisches Institut, Universität Heidelberg, Im Neuenheimer Feld 253, D-69120 Heidelberg, Germany

Received 16 January 2001

Abstract

Chlorine atom spin–orbit product branching ratios and total absolute reaction cross-sections have been measured for the H + DCl → HD + Cl gas-phase reaction for collision energies of $E_{col} = 1.0$, 1.4 and 1.7 eV. The measured $Cl^*(^2P_{1/2})$ atom spin–orbit product branching ratios $\phi_{Cl^*}(1.0\ eV) = [Cl^*]/[Cl + Cl^*] = (0.06 \pm 0.02)$, $\phi_{Cl^*}(1.4\ eV) = (0.07 \pm 0.01)$, and $\phi_{Cl^*}(1.7\ eV) = (0.16 \pm 0.01)$ revealed the increasing importance of a non-adiabatic reaction channel H + DCl → HD + Cl^* with increasing collision energy. The measured total absolute reaction cross-sections allow for comparison with results from recent quasi-classical trajectory (QCT) calculations [F.J. Aoiz et al. J. Phys. Chem. A 104 (2000) 10452].

1. Introduction

The gas-phase reaction of hydrogen atoms with hydrogen chloride

$$H + HCl \rightarrow H_2 + Cl \quad (1)$$

has played an important role in the development of modern chemical kinetics, see e.g. [1]. Since the pioneering experimental work of Bodenstein and Dux [2,3] on the (H_2/Cl_2)-system – which finally established for that system the presence of a chain mechanism in which Cl atoms act as chain carriers [4] – a large number of kinetic studies were carried out for the H + HCl elementary reaction, see e.g. [5] including state-selected experiments with vibrational excited HCl reagent molecules [6]. Besides the kinetic studies several experimental studies on the dynamics of the H + HCl → H_2 + Cl abstraction reaction employing translational excited H atoms in combination with state-resolved detection of the H_2 product molecules using coherent anti-Stokes Raman scattering (CARS) [7,8] and vacuum ultraviolet laser induced fluorescence (VUV-LIF) detection of ground-state $Cl^*(^2P_{3/2})$ atom products, respectively, were reported [9]. The most recent experimental and theoretical studies [10] demonstrated that there is no sharp increase in the absolute reaction cross-section as a function of collision energy in the range $E_{col} = 1.0$–1.7 eV as it was suggested by the earlier reaction dynamic experiments [7,9]. In [10], it could be further shown that at higher collision energies appreciable amounts of spin–orbit excited $Cl^*(^2P_{1/2})$ atom

* Corresponding author. Fax: +49-6221-545-050.

E-mail address: aw2@ix.urz.uni-heidelberg.de (H.-R. Volpp).

[1] On sabbatical leave from the Radiation Chemistry and Chemical Dynamics Division, Bhabha Atomic Research Centre, Mumbai 400 085, India.

0009-2614/01/$ - see front matter
PII: S0009-2614(01)00380-3

products are formed via a non-adiabatic reaction channel in the H + HCl reaction. For the isotopic analogue to this reaction, H + DCl, however, no detailed information about the corresponding non-adiabatic reaction channel $H + DCl \rightarrow HD + Cl^*(^2P_{1/2})$ is available so far. Although Polanyi and co-workers could measure absolute reaction cross-section for the adiabatic abstraction channel $H + DCl \rightarrow HD + Cl(^2P_{3/2})$ at different collision energies, the formation of $Cl^*(^2P_{1/2})$ product atoms could not be observed [11]. The present work represents an extension of the latter studies towards the characterization of the collision energy dependence of the adiabatic versus non-adiabatic abstraction reaction product branching and the determination of total (adiabatic and non-adiabatic) absolute reaction cross-sections at three additional collision energies (1.0, 1.4 and 1.7 eV). The latter values allow for comparison with recent quasi-classical trajectory (QCT) calculations [10] carried out on the G3 [12] and BW1/BW2 [13] potential energy surfaces (PESs), respectively.

2. Experimental

The experiments were carried out in a flow reactor with a crossed laser beam 'pump' and 'probe' setup similar to the one used in our previous H + HCl reaction dynamic studies [9,10]. H atom precursors H_2S (UCAR electronic grade, 99.99%) and HBr (Messer Griesheim, 99.8%), respectively, were pumped through the reactor together with room temperature DCl (Sigma Aldrich, D > 99%). The ratios of [H_2S]:[DCl] and [HBr]:[DCl] were typically 1:2 at a total pressure between 40 and 100 mTorr. As in our previous $H + D_2$ dynamics studies which were carried out in flowing H_2S/D_2 and HCl/D_2 mixtures [14], the H_2S and HBr were mixed with the DCl flow just before entering the reaction cell in order to prevent isotope scrambling.

Two different excimer lasers with pulse durations of typically 10–15 ns operated with different gas mixtures were employed as photolysis (pump) lasers. One laser operating with a KrF gas mixture ($\lambda_{pump} = 248$ nm) was used to photodissociate H_2S generating translationally energetic H atoms with an average collision energy of $E_{col} = 1.0$ eV in the (H–DCl)-center-of-mass system. A second one operating with a KrCl gas mixture ($\lambda_{pump} = 222$ nm) was used to photodissociate H_2S and HBr, respectively, providing translationally energetic H atoms with average collision energies of $E_{col} = 1.4$ eV and $E_{col} = 1.7$ eV with energy spreads of about 10%. Pump laser intensities employed in the experiments were in the range 2–12 mJ/cm^2.

Pulsed narrow-band VUV-probe laser radiation (pulse duration 10–15 ns; band width $\Delta\omega_{probe} \approx 0.3$ cm^{-1}), tunable in the wavelength region 133.5–136.4 nm, was generated using the Wallenstein method for resonant third-order sum-difference frequency conversion ($\omega_{probe} = 2\omega_R - \omega_T$) of pulsed dye laser radiation in Krypton [15]. In the four-wave mixing process the frequency ω_R ($\lambda_R = 212.55$ nm) is two-photon resonant with the Kr 4p–5p (1/2,0) transition. The frequency ω_T could be tuned from 480 to 521 nm to cover the four allowed $Cl(4s^2P_{j'} \leftarrow 3p^2P_{j''}; j' = 1/2, 3/2 \leftarrow j'' = 1/2, 3/2)$ transitions. Ground-state $Cl(^2P_{3/2})$ and spin–orbit excited-state $Cl^*(^2P_{1/2})$ atoms ($\Delta E_{so} = E(^2P_{1/2}) - E(^2P_{3/2}) = 881$ cm^{-1}) were detected using the $(j' = j'')$-transitions, which have the highest transition probabilities $f_{3/2,3/2} = 0.114$ and $f_{1/2,1/2} = 0.088$, respectively [16].

The fundamental laser radiation was obtained from two tunable dye lasers, simultaneously pumped by a XeCl excimer laser, one of which, ω_R, was obtained by frequency doubling using a BBO II crystal. The generated VUV-light was carefully separated from the fundamental laser radiation by a lens monochromator (see [9, Fig. 1]). The probe beam was aligned to overlap the photolysis beam at right angles in the viewing region of a LIF detector. Delay times between pump and probe laser pulses were typically between 100 ± 5 and 200 ± 5 ns allowing the collision-free detection of the nascent Cl and Cl^* atom reaction products. Under these experimental conditions relaxation of Cl^* by quenching was negligible. Cl and Cl^* LIF signals were measured through a band pass filter (ARC model 130-B-1D with a transmission 29% at 134 nm) by a solar blind photomultiplier (THORN EMI model 9413 B). In order to obtain

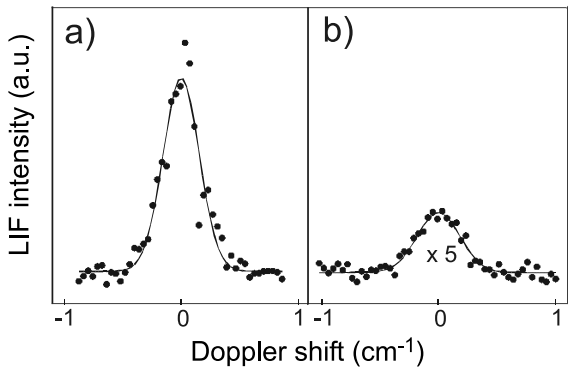

Fig. 1. Doppler profiles of Cl (a) and Cl^* (b) product atoms observed in the 222 nm photolysis of a 1:2 mixture of H_2S and DCl ($p_{tot} = 60$ mTorr; $\Delta t = 150$ ns). The measured laser induced fluorescence excitation spectra (represented by the solid cirlces) are plotted against the wavenumber mismatch in units of cm^{-1}. Line centers correspond to the ($4s^2P_{j'=3/2} \leftarrow 3p^2P_{j''=3/2}$) transition of the Cl atom (74225.8 cm^{-1}) and to the ($4s^2P_{j'=1/2} \leftarrow 3p^2P_{j''=1/2}$) transition of the Cl^* atom (73983.1 cm^{-1}), respectively. The solid lines represent results of a least-square fit using a Gaussian function.

a satisfactory S/N ratio, each point of the Cl and Cl^* atom Doppler profiles shown in Fig. 1 was typically averaged over 30 laser shots. Experiments were carried out at a laser repetition rate of 6 Hz. As in our previous studies of the H + HCl reaction it was found that the VUV probe beam itself produced small Cl/Cl^* atom LIF signals via photolysis of DCl. In order to subtract these 'background' Cl/Cl^* atoms from the Cl/Cl^* atoms produced in the H + DCl reaction an electronically controlled mechanical shutter was inserted into the pump laser beam path (for details see [9,10]). At each point of the Cl and Cl^* atom line scan, the signal was first averaged with the shutter opened and again averaged with the shutter closed. A point- by-point subtraction procedure was adopted, to obtain directly and on-line a signal free from 'probe-laser-generated' background Cl and Cl^* atoms.

3. Results and discussion

Doppler profiles of ($^2P_{3/2}$) ground-state Cl atoms and ($^2P_{1/2}$) spin–orbit excited Cl^* atoms produced in the H + DCl reaction at $E_{col} = 1.4$ eV are depicted in Fig. 1. The spin–orbit branching ratio, $\phi_{Cl^*}(1.4\text{ eV}) = [Cl^*]/[Cl + Cl^*] = 0.07 \pm 0.01$, for Cl^* atom product formation was determined from the integrated areas of the corresponding Doppler profiles after correcting for the different oscillator strengths of the spectral transitions which were used to probe the two different fine-structure states. The quoted error represents the $\pm 1\sigma$ statistical uncertainty obtained in the evaluation of the experimental data (eight sets of Cl and Cl^* Doppler profiles were evaluated). The value of the spin–orbit branching ratio is depicted in Fig. 2 together with the two other values obtained in the present study: $\phi_{Cl^*}(1.0\text{ eV}) = [Cl^*]/[Cl + Cl^*] = 0.06 \pm 0.02$, $\phi_{Cl^*}(1.7\text{ eV}) = 0.16 \pm 0.01$. In a previous dynamics study of the H + DCl reaction [11] an upper limit for the Cl^* formation cross-sections in the collision energy range $E_{col} = 1.2$–1.8 eV was reported which corresponds to an approximately constant value of $\phi_{Cl^*} \approx 0.1$. The present results, however, clearly indicate that the relative contribution of the non-adiabatic abstraction reaction channel H + DCl → HD + Cl^* exhibits a significant increase with increasing collision energy. Within the combined error bars the present results are in agreement with the collision energy dependence of the Cl atom spin–orbit branching ratio determined for the H + HCl reaction [10].

To the best of our knowledge no dynamical calculations were carried out so far which take into

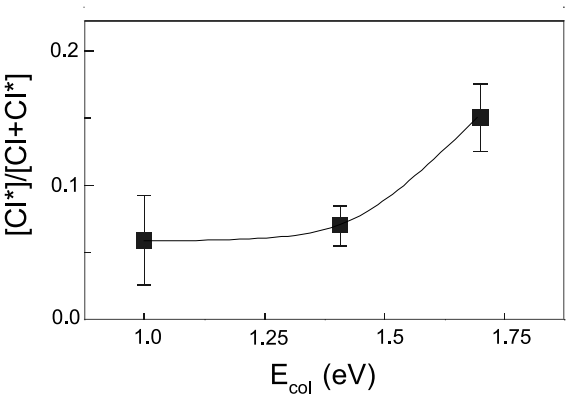

Fig. 2. Dependence of the measured Cl^* atom product spin–orbit branching ratio $[Cl^*]/[Cl + Cl^*]$ on the H + DCl reagent collision energy. The solid line is drawn just to guide the eye.

account the multi-surface nature of the H + HCl/DCl abstraction reactions. However, the Cl^* product formation dynamics and its collision energy dependence as observed in the present studies can be rationalized in the framework of a reaction mechanism originally proposed by Liu and co-workers to explain the results of their $Cl^* + H_2 \rightarrow H + HCl$ reactive scattering experiments [17]. In the latter experiments it was observed that Cl^* atoms are by a factor of ~6 more reactive to H_2 than ground-state Cl atoms. The enhanced reactivity of Cl^* atoms towards H_2 was attributed to non-adiabatic transitions from the initially populated non-reactive $(2^2A')$-PES to the ground $(1^2A')$-PES which correlates with H + HCl ground-state products and it was postulated that these non-adiabatic transitions take place predominately near the avoided-crossing region at bent Cl–HH geometries in the $Cl + H_2$ entrance channel. For the $H + HCl \rightarrow H_2 + Cl$ abstraction reaction, on the other hand, it has been demonstrated that for low collision energies, $E_{col} \approx 0.7$ eV, the reaction products are almost exclusively backward scattered indicating a direct rebound-type mechanism [8]. These restriction to collinear H–HCl approach geometries at low collision energies was attributed to the strongly repulsive H–H–Cl bending potential which leads to a sharp increase of the reaction barrier height for approach geometries deviating from the collinear one. At higher collision energies ($E_{col} \geqslant 1.6$ eV), however, significant contributions due to non-collinear reactive collisions became noticeable. Therefore, the increase in the Cl^* spin–orbit branching ratio as observed in the present work (see Fig. 2) for the H + DCl reaction could be explained by an increase in the reaction probability for non-collinear reagent geometries at higher collision energies which could promote the occurrence of non-adiabatic transitions between the $(1^2A')$ H–DCl-PES – which correlates with HD + Cl products – and the $(2^2A')$-PES – which correlates with $HD + Cl^*$ products – in the exit channel of the abstraction reaction pathway.

Total absolute reaction cross-sections for the $H + DCl \rightarrow HD + Cl$ abstraction reaction at $E_{col} = 1.0$, 1.4 and 1.7 eV were obtained by means of a calibration method using the $H + HCl \rightarrow H_2 + Cl$ reaction, for which total absolute reaction cross-sections were reported in [9,10] as a reference. By comparing the Cl atom signal $S_{Cl}(H + DCl)$ – defined as the area below the Cl atom Doppler profile – produced in the H + DCl reaction with the corresponding Cl atom signal $S_{Cl}(H + HCl)$ produced in the H + HCl reaction (see Fig. 3) the total absolute reaction cross-section σ_R for the H + DCl reaction can be obtained using the following formula:

$$\sigma_R = \frac{S_{Cl}(H + DCl)}{S_{Cl}(H + HCl)} \times \frac{\phi_{Cl}(H + HCl)}{\phi_{Cl}(H + DCl)} \times \frac{v_{rel}(H + DCl)}{v_{rel}(H + HCl)} \times \sigma_R(H + HCl). \quad (2)$$

Here $v_{rel}(H + HCl)$ and $v_{rel}(H + DCl)$ are the relative velocities of the H + HCl and H + DCl reactant pairs. $\phi_{Cl}(H + HCl)$ and $\phi_{Cl}(H + DCl)$ are the Cl ground-state atom spin–orbit branching ratios $[Cl]/[Cl + Cl^*]$ obtained in the H + HCl and H + DCl reaction measurement, respectively. In Eq. (2), $\sigma_R(H + HCl)$ stands for the total reaction cross-section of the H + HCl abstraction reaction for which absolute values have been reported for collision energies of 1.0, 1.4 and 1.7 eV [9,10].

To determine total absolute reactive cross-sections for the H + DCl abstraction reaction in a

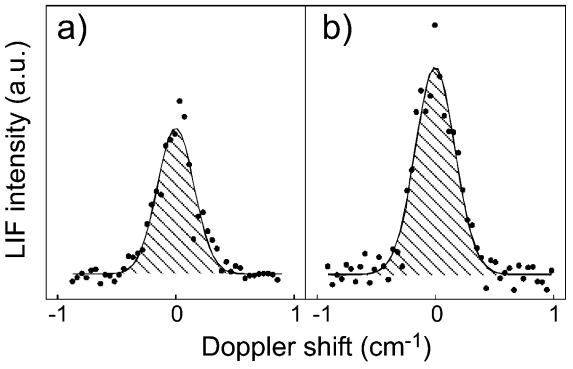

Fig. 3. Comparison between the integrated LIF intensity of Cl atoms produced in the H + DCl reaction (a) with the integrated LIF intensity of Cl atoms produced in the H + HCl reaction (b) at $E_{col} = 1.4$ eV. Doppler profiles shown in (a) and (b) were recorded under the same experimental conditions as the Doppler profiles shown in Fig. 1. Line centers correspond to the $(4s^2P_{j'=3/2} \leftarrow 3p^2P_{j''=3/2})$ transition of the Cl atom (74225.8 cm^{-1}).

number of experimental runs, integrated areas under the Cl fluorescence excitation spectra were determined under identical experimental conditions for the H + DCl and the H + HCl reaction. Using Eq. (2) the evaluation of the experimental data yielded the following values for the total reaction cross-sections of the H + DCl abstraction reaction: $\sigma_R(1.0\ \text{eV}) = (0.27 \pm 0.06)\ \text{Å}^2$, $\sigma_R(1.4\ \text{eV}) = (0.22 \pm 0.09)\ \text{Å}^2$ and $\sigma_R(1.7\ \text{eV}) = (0.10 \pm 0.05)\ \text{Å}^2$. The quoted experimental errors were calculated from the individual errors of the entries of Eq. (2) on the basis of simple error propagation.

In Fig. 4, the reaction cross-sections for the H + DCl abstraction reaction obtained in the present study are shown (solid triangles) together with previous results (solid circles) [11]. For comparison, cross-sections obtained in QCT calculations on the G3 (solid line) [18] and on the new BW1 (dot-dash line) and BW2 (dashed line) PESs [10] are also included. To allow for comparison with the experiments the QCT cross-sections have been calculated for a $T = 300$ K distribution of DCl ($v = 0$) reagent rotational levels [10,18]. As can be seen in Fig. 4, reaction cross-sections obtained on the BW1 PES are slightly smaller than the BW2 ones due to the slightly lower barrier of the latter PES. The BW1, BW2, and G3 excitation functions, $\sigma_R(E_{col})$, are quite similar in shape, however, for $E_{col} > 0.25$ eV the G3 one is considerably smaller in absolute value and is therefore in much better agreement with the present as well as with the earlier experimental results of Polanyi and coworkers [11].

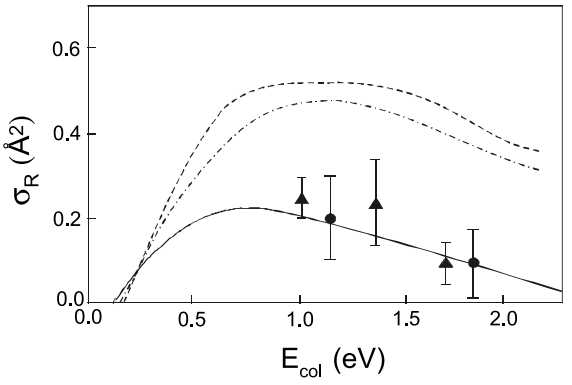

Fig. 4. Reaction cross-section as a function of collision energy for the H + DCl → HD + Cl reaction. The symbols represent experimentally measured reaction cross-sections. Solid triangles correspond to the results of the present study, solid circles are the results of [11]. The lines represent excitation functions obtained in quasi-classical trajectory calculations carried out on the G3 (solid line), BW1 (dot-dash line) and BW2 (dashed line) PESs [18,10].

The origin of the large difference in reactivity observed in the QCT calculations on the BW2 and the G3 PES has been investigated in detail [10]. By analyzing individual trajectories in combination with R–γ contour plots of the PESs (R denotes the distance between the incoming H atom and the center-of-mass of the DCl molecule and γ is the Jacobi angle between R and the DCl internuclear distance) it could be shown that narrow 'reactive valleys' in the contour plot of the BW2 PES centered at $\gamma \approx 30°$ (which are not present in the G3 PES) are responsible for the higher reactivity of the abstraction pathway observed on the BW2 PES (see [10, Fig. 7]).

4. Summary and conclusion

Cl atom spin–orbit branching ratios for the H + DCl → HD + Cl gas-phase reaction have been measured as a function of collision energy in the range $E_{col} = 1.0$–1.7 eV which demonstrate the increasing importance of the electronically nonadiabatic reaction channel H + DCl → HD + Cl* with increasing collision energy. The experimentally measured absolute reaction cross-sections were found to be in good agreement with previous measurements at different collision energies [11] and with the results of QCT calculations on the G3 PES [18]. The experimental reaction cross-sections, however, are more than a factor of two smaller than the cross-sections obtained in QCT calculations on the new BW2 PES. At this point it should be noted that although the latter PES is based on high-quality ab initio data and should therefore be more accurate than the earlier partly semi-empirical G3 PES, spin–orbit coupling effects are not included in the BW2 PES while they are approximately included in the G3 PES. This together with the fact that the theoretical reaction cross-sections

shown in Fig. 4 were obtained in QCT calculations which were purely adiabatic [10,18] prevents at the present stage to draw a final conclusion regarding the comparative quality of these two PESs. As it has been shown experimentally in the present work, non-adiabatic transitions readily occur in the abstraction reaction at high enough collision energies. Therefore – as already noted by Polanyi and co-workers [11] – a more sophisticated theoretical treatment beyond the Born–Oppenheimer approximation, e.g., multi-surface scattering calculations taking into account the coupling to the upper $(2^2A')$-PES, is clearly needed for a more quantitative description of the dynamics of the H + DCl reactions. In the light of the flourishing of experimental and theoretical studies of the dynamics of the H + DCl/HCl [6–11,18] and $Cl/Cl^* + H_2/D_2/HD$ [17,19–23] reactions it can be expected that they will soon become important benchmark systems in electronically non-adiabatic chemistry [24].

Acknowledgements

The present work was supported by the Deutsche Forschungsgemeinschaft (DFG). Partial support received in the framework of the German–Spanish scientific exchange program 'Acciones Integradas' (HA-1999-0050) and by the DLR Bonn (Indo-German bilateral agreement, project IND 99/050) is also gratefully acknowledged. A.L. was supported by the Landesgraduierten Förderung Baden-Württemberg. HRV thanks F.J. Aoiz, V.J. Herrero, and I. Tanarro for helpful discussions. The authors would like to dedicate this article to Prof. Dr. Dres. h.c. Jürgen Troe on the occasion of his 60th birthday.

References

[1] T.C. Allison, S.L. Mielke, D.W. Schwenke, G.C. Lynch, M.S. Gordon, D.G. Truhlar, in: J. Wolfrum, H.-R. Volpp, R. Rannacher, J. Warnatz (Eds.), Gas Phase Chemical Reaction Systems: Experiments and Models 100 Years after Max Bodenstein, Springer Series in Chemical Physics Vol. 61, Springer, Heidelberg, 1996, p. 111.
[2] M. Bodenstein, W. Dux, Z. Phys. Chem. 85 (1913) 297.
[3] K.J. Laidler, Chemical Kinetics, Harper & Row, New York, 1987, and references therein.
[4] W. Nernst, Z. Elektrochem. 24 (1918) 335.
[5] R. Atkinson, D.L. Baulch, R.A. Cox, R.F. Hampson, J.A. Kerr, M.J. Rossi, J. Troe, J. Phys. Chem. Ref. Data 26 (1997) 521, and references therein.
[6] J. Wolfrum, in: A. Fontijn, M.A.A. Clyne (Eds.), Reactions of Small Transient Species, Academic Press, New York, 1983, p. 105.
[7] P.M. Aker, G.J. Germann, J.J. Valentini, J. Chem. Phys. 90 (1989) 4795.
[8] P.M. Aker, J.J. Valentini, Isr. J. Chem. 30 (1990) 157.
[9] R.A. Brownsword, C. Kappel, P. Schmiechen, H.P. Upadhaya, H.-R. Volpp, Chem. Phys. Lett. 289 (1998) 241.
[10] F.J. Aoiz, L. Bañares, T. Bohm, A. Hanf, V.J. Herrero, K.-H. Jung, A. Läuter, K.W. Lee, M. Menéndez, V. Sáez Rábanos, I. Tanarro, H.-R. Volpp, J. Wolfrum, J. Phys. Chem. A 104 (2000) 10452.
[11] V.J. Barclay, B.A. Collings, J.C. Polanyi, J.H. Wang, J. Phys. Chem. 95 (1991) 2921.
[12] T.C. Allison, G.C. Lynch, D.G. Truhlar, M.S. Gordon, J. Phys. Chem. 100 (1996) 13575.
[13] W. Bian, H.-J. Werner, J. Chem. Phys. 112 (2000) 220.
[14] R.A. Brownsword, M. Hillenkamp, T. Laurent, H.-R. Volpp, J. Wolfrum, R.K. Vatsa, H.-S. Yoo, J. Phys. Chem. 101 (1997) 6448.
[15] G. Hilber, A. Lago, R. Wallenstein, J. Opt. Soc. Am. B 4 (1987) 1753.
[16] W.L. Wiese, M.W. Smith, B.M. Miles, Atomic Transition Probabilities, Natl. Bur. Stand. Ref. Data Ser., Natl. Bur. Stand. (US) Circ. No. 22 (US GPO, Washington DC 1969).
[17] S.-H. Lee, K. Liu, J. Chem. Phys. 111 (1999) 6253.
[18] F.J. Aoiz, L. Bañares, J. Phys. Chem. 100 (1996) 18108.
[19] M. Alagia, N. Balucani, L. Cartechini, P. Casavecchia, E.H. van Kleef, G.G. Volpi, F.J. Aoiz, L. Bañares, D.W. Schwenke, T.C. Allison, S.L. Mielke, D. Truhlar, Science 73 (1996) 1519.
[20] D. Skouteris, D.E. Manolopoulos, W. Bian, H.-J. Werner, L.-H. Lai, K. Liu, Science 286 (1999) 1713.
[21] S.-H. Lee, L.-H. Lai, K. Liu, H. Chang, J. Chem. Phys. 110 (1999) 8229.
[22] P. Casavecchia, L. Cartechini, F.J. Aoiz, Faraday Discuss. 113 (1999) 201.
[23] S.A. Kandel, A.J. Alexander, Z.H. Kim, R.N. Zare, F.J. Aoiz, L. Bañares, J.F. Castillo, V. Sáez Rábanos, J. Chem. Phys. 112 (2000) 670.
[24] D.R. Yarkony, J. Phys. Chem. 100 (1996) 18162.